2009 International Symposium on Nonlinear Theory and its Applications
NOLTA'09, Sapporo, Japan, October 18-21, 2009

Inter-spike Interval Characteristics of Chaotic Spiking Oscillators

Yusuke Matsuoka†, Tomonari Hasegawa†† and Toshimichi Saito†††

†ECE Dept., Yonago National College of Technology, 4448, Hikona-cho, Yonago-shi, Tottori, Japan.
††Uniden Co., Ltd., Tokyo, Japan.
†††EE Dept., Hosei University, 3-7-2, Kajino-cho, Koganei-shi, Tokyo, Japan.
Email: †ymatuoka AT yonago-k.ac.jp, †††tsaito AT hosei.ac.jp

Abstract—This paper considers dynamics of two simple chaotic spiking oscillators (CSOs). The CSOs repeat vibrate-and-fire dynamics and can exhibit various chaotic/periodic spike-trains. The CSO with piecewise linear vector field has "isochronism" property and inter-spike interval spectrums can have narrow-bands discretely. The CSO with piecewise constant vector field does not have "isochronism" property and inter-spike interval spectrums can have a wide-band.

1. Introduction

An integrate-and-fire switch (IFS) is a key element and can cause a variety of nonlinear phenomena. Various spiking neuron models include the IFS that causes reset of a state variable to a base level. Repeating such operation, the spiking neuron models exhibit various spike-trains [1]-[2]. Pulse-coupled neural networks and signal/image processing are studied based on spiking neuron models and spike-trains [3]-[5]. Analysis of dynamics including the IFS and spike-trains are important for both fundamental nonlinear problem and consideration of engineering applications.

This paper studies chaotic spiking oscillators (CSOs) [6], [7]. The CSOs have two state variables that can vibrate divergently. If one state reaches a threshold level, the IFS is occurred and the state is reset to a base level instantaneously. The CSOs then output a spike. Repeating the vibrate-and-fire dynamics, the CSOs can output spike-trains.

First, we consider the CSO with piecewise liner vector field (PWL-CSO). The trajectory of the PWL-CSO is piecewise smooth and can draw unstable spirals in the phase plane. The PWL-CSO exhibits periodic/chaotic attractors and spike-trains. In order to clarify characteristics of spike-trains, we show inter-spike intervals (ISIs) spectrums and distribution in numerical simulations. Focusing on switching moment, we can derive an 1-D return map and can analyze the dynamics precisely.

Second, we consider the CSO with piecewise constant vector field (PWC-CSO). The trajectory is PWL and can draw unstable rectangular spirals in the phase plane. The PWC-CSO exhibits only chaotic attractor and spike-trains. In numerical simulations, we show ISI spectrums and distribution. Since the trajectory is PWL, the return map is PWL and we can analyze the dynamics theoretically [8].

We have found properties of the two CSOs as the following. (1) The PWL-CSO has "isochronism" with respect to vibration of the state whereas the PWC-CSO does not have the isochronism. (2) As the parameter varies, the PWL-CSO can exhibit periodic spike-trains with line spectrum. The PWC-CSO can exhibit chaotic spike-trains with line-like spectrum [9]. (3) The PWC-CSO can have wide-band ISI spectrum whereas the PWL-CSO can not have wide-band but narrow bands ISI spectrums.

Dynamics of the CSOs have been studied in [9], [10], but these papers have not been discussed the comparison between the two CSOs and ISI characteristics.

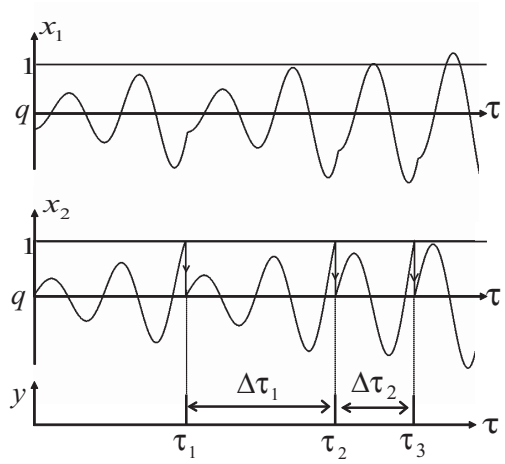

Figure 1: Dynamics of the PWL-CSO for $a = 0.2$ and $q = 0$.

2. Piecewise Linear Chaotic Spiking Oscillator

We consider dynamics of the PWL-CSO. The dynamics can be described as the following equation:

$$\begin{cases} \dot{x}_1 = x_2 \\ \dot{x}_2 = ax_2 - x_1 \end{cases} \quad \text{for } x_2(\tau) < 1, \tag{1}$$

$$(x_1(\tau_+), x_2(\tau_+)) = (x_1(\tau), q) \text{ if } x_2(\tau) = 1, \tag{2}$$

where "$\cdot$" denote differentiation by dimensionless time τ. x_1 and x_2 are dimensionless state variables, respectively. This equation has two parameters a and q. For simplicity, we assume $0 < a < 2$ and $-1 < q < 1$. In this case, Eq.

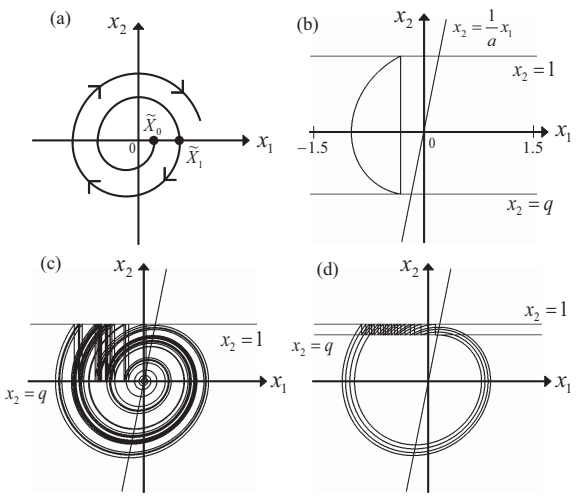

Figure 2: Trajectory and attractors for $a = 0.2$ in the phase space. (a) Typical trajectory for $x_2 < 1$, (b) Periodic attractor for $q = -0.81$, (c) Chaos for $q = 0$, (d) Chaos for $q = 0.81$.

(1) has unstable complex eigenvalues and the states x_1 and x_2 can vibrate divergently as shown in Fig. 1. If x_2 reaches threshold 1, x_2 is reset to base q instantaneously holding continuity property of x_1. The PWL-CSO then outputs a spike $y = 1$:

$$y(\tau_+) = \begin{cases} 1 & \text{if } x_2(\tau) = 1 \\ 0 & \text{otherwise.} \end{cases} \tag{3}$$

Repeating vibrate-and-fire dynamics, the PWL-CSO outputs various spike-trains $y(\tau)$. The PWL-CSO exhibits chaotic/periodic attractors as shown in Fig. 2. When the trajectory draws unstable spiral as shown in Fig. 2 (a), let a trajectory start from $\tilde{X}_0$ on positive x_1-axis at $\tau = 0$. It returns to the positive x_1-axis at point $\tilde{X}_1$. Let T be time of "one cycle" from a start point $\tilde{X}_0$ to a return point $\tilde{X}_1$ on positive x_1-axis. The rotation time T is constant and the PWL-CSO has the "isochronism" property.

Let τ_n be the n-th firing time and ISI $\Delta\tau_n$ as shown in Fig. 1. The n-th ISI can be given by $\Delta\tau_n = \tau_{n+1} - \tau_n$ where n is a positive integer. Fig. 3 shows ISI spectrums corresponding to Fig. 2 (b) to (d). Fig. 4 shows a diagram of distribution of the ISIs. As q approaches 0, the maximal length of the ISIs becomes long. As q approaches 1, the maximal length of the ISIs becomes short. The PWL-CSOs exhibits periodic attractor and has line spectrum, approaching to $q = -1$.

In order to analyze the dynamics precisely, we derive an 1-D return map. Let $L_q = \{(x_1, x_2) \mid x_2 = q\}$ and let a point on L_q be represented by its x_1-coordinate. Let us consider the trajectory that is reset to a point X_0 on L_q at the first firing time τ_1 as shown in Fig. 5. The trajectory vibrates below the threshold and resets to a point X_1 on L_q at the second firing time τ_2. Let X_0 and X_1 be the first and second reset points, respectively. Since X_0 determines X_1, we can define the 1-D return map:

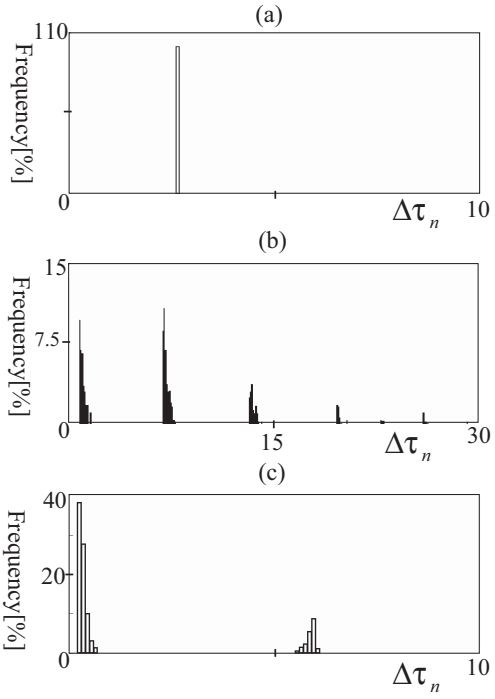

Figure 3: ISI spectrums for $a = 0.2$. Number of spikes = 10000. (a) $q = -0.81$, (b) $q = 0$, (c) $q = 0.81$. Fig. (a) to (c) correspond to Fig. 2 (b) to (d).

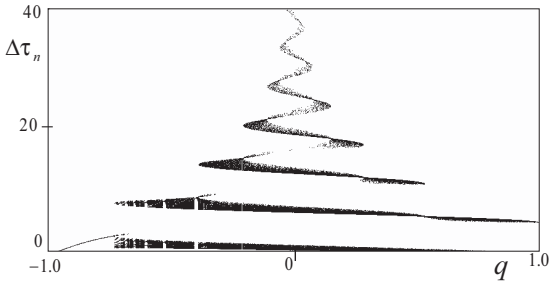

Figure 4: Distribution of the ISIs for $a = 0.2$.

$$F : L_q \to L_q, \quad X_0 \mapsto X_1. \tag{4}$$

Fig. 6 shows the return maps corresponding to Fig. 2 (b) and (d).

3. Piecewise Constant Chaotic Spiking Oscillator

In this section, we consider dynamics of the PWC-CSO that is given by applying signum function to the right-hand sides of the first and second lines of Eq. (1).

$$\begin{cases} \dot{x}_1 = \mathrm{sgn}(x_2) \\ \dot{x}_2 = \mathrm{sgn}(ax_2 - x_1) \end{cases} \quad \text{for } x_2(\tau) < 1 \tag{5}$$

$$\mathrm{sgn}(x) = \begin{cases} 1 & \text{for } x > 0 \\ 0 & \text{for } x = 0 \\ -1 & \text{for } x < 0 \end{cases}$$

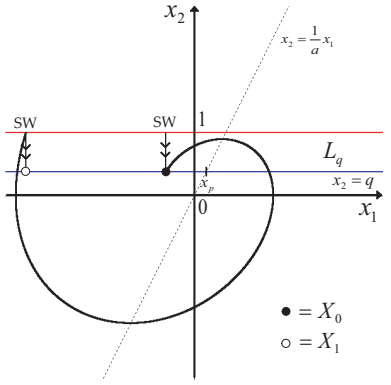

Figure 5: Definition of the return map.

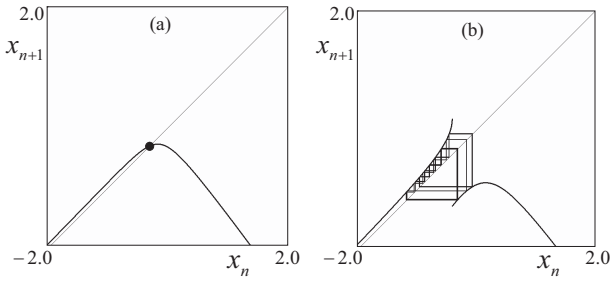

Figure 6: Typical return maps for $a = 0.2$. (a) Stable fixed point for $q = -0.81$, (b) Chaos for $q = 0.81$. Fig. (a) and (b) correspond to Fig. 2 (b) and (d).

$$(x_1(\tau_+), x_2(\tau_+)) = (x_1(\tau), q) \ \text{ if } \ x_2(\tau) = 1. \qquad (6)$$

The dimensionless equation has two parameters a and q where $0 < a < 1$ and $-1 < q < 1$ for simplicity. Since the equation has PWC vector fields, the trajectory is PWL. When $0 < a < 1$, the trajectory can vibrate divergently and can draw rect-spiral as shown in Fig. 7 and Fig. 8 (a), respectively. When the trajectory draws unstable rect-spiral, let a trajectory start from $\tilde{X}_0$ on positive x_1-axis at $\tau = 0$. It returns to a point $\tilde{X}_1$ on positive x_1-axis at time T. $\tilde{X}_1$ and the rotation time T is given by

$$\tilde{X}_1 = \alpha^2 \tilde{X}_0, \ \ T = (\alpha^2 - 1) a \tilde{X}_0, \ \ \alpha \equiv \frac{a+1}{a-1}. \qquad (7)$$

That is, T depends on starting point $\tilde{X}_0$ and the PWC-CSO has an important property "non-isochronism". Repeating the vibrate-and-fire dynamics, the PWC-CSO exhibits chaotic attractors and spike-trains as shown in Fig. 8. We show the ISI spectrums in Fig. 9 corresponding to FIg. 8 (b) to (d). The PWC-CSO has various type of the ISI spectrums. As q approaches 1, the ISI $\Delta_{\tau_n} = 1 - q$ dominates. Fig. 10 shows the diagram of distribution of the ISI. In the PWC-CSO, only chaotic spike-trains exist. As q approaches 0, the ISI distribution becomes wide-band.

Using the similar consideration as the PWL-CSO, we can derive an 1-D return map $F : L_q \to L_q, \ \ X_0 \mapsto X_1$. Fig. 11 shows typical return maps corresponding to Fig. 8

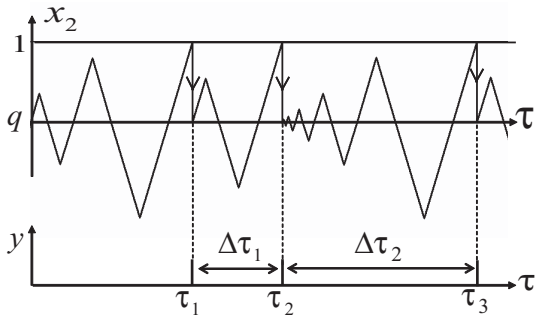

Figure 7: Dynamics of the PWC-CSO for $a = 0.2$ and $q = 0$.

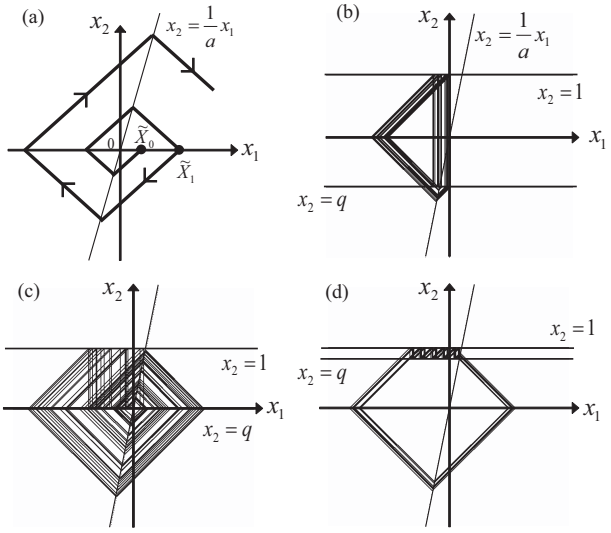

Figure 8: Trajectory and attractors of the PWC-CSO for $a = 0.2$. (a) Typical trajectory for $x_2 < 1$, (b) Chaos for $q = -0.81$, (c) Chaos for $q = 0$, (d) Chaos for $q = 0.81$.

(b) and (d). The map is PWL and theoretical evidence for chaos generation can be found in [7].

4. Comparison between the two CSOs

We describe the comparison between the two CSOs as the following.

(A) Trajectory and attractor

The PWL-CSO has the "isochronism" property and can exhibit chaotic/periodic attractors. However, the PWC-CSO has "non-isochronism" and exhibits only chaotic attractor (see Fig. 2 and Fig. 8).

(B) ISI spectrums

When $q = 0$, the ISI spectrums of the PWL-CSO can have some narrow-bands discretely whereas the PWC-CSO has continuous wide-band spectrum. (see Fig. 3 and Fig. 9).

(C) ISI distribution

Around $q = 0$ in the PWL-CSO, long length of the ISI can appear. For $q = 0$, especially, the maximal length of the ISI becomes infinitely. In the PWC-CSO, however, the ISI

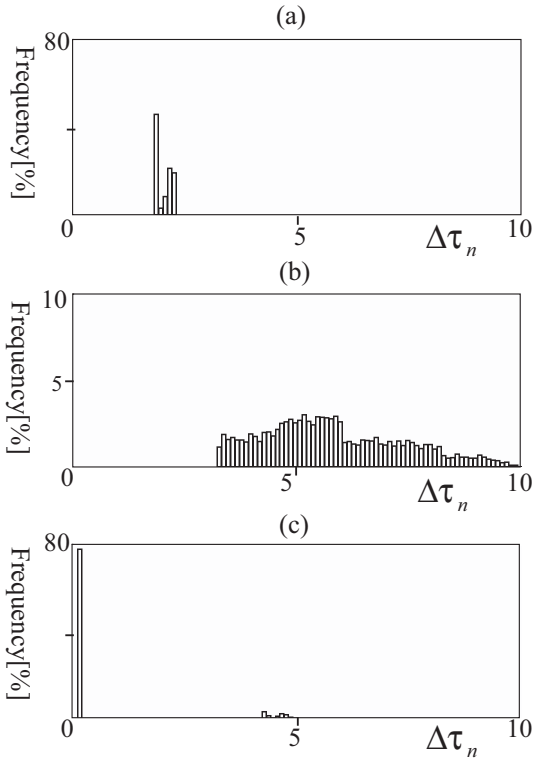

Figure 9: ISI spectrums of the PWC-CSO for $a = 0.2$. Number of spikes = 10000. (a) $q = -0.81$, (b) $q = 0$, (c) $q = 0.81$. Fig. (a) to (c) correspond to Fig. 8 (b) to (d).

is finite length (see Fig. 4 and Fig. 10). For $q > 0$, the PWL-CSO exhibits chaos and window alternatively [10] whereas the PWC-CSO exhibits chaos and island with line-like spectrum alternatively [9].

5. Conclusions

We have studied dynamics of the two CSOs. We have clarified ISIs characteristics and have compared between the two CSOs. Future problems include detailed analysis for bifurcation, comparison for wider parameter regions and consideration for spike-based engineering applications.

References

[1] J. P. Keener, F. C. Hoppensteadt & J. Rinzel, "Integrate-and-fire models of nerve membrane response to oscillatory input," SIAM J. Appl. Math., 41, pp. 503-517, 1981.

[2] E. M. Izhikevich, "Simple Model of Spiking Neurons," IEEE Trans. Neural Networks, 14, pp. 1569-1572, 2003.

[3] S. R. Campbell, D. Wang and C. Jayaprakash, "Synchrony and desynchrony in integrate-and-fire oscillators," Neural computation, vol. 11, pp. 1595-1619, 1999.

[4] H. Nakano and T. Saito, "Grouping synchronization in a pulse-coupled network of chaotic spiking oscillators," IEEE Trans. Neural Networks, 15, 5, pp. 1018-1026, 2004.

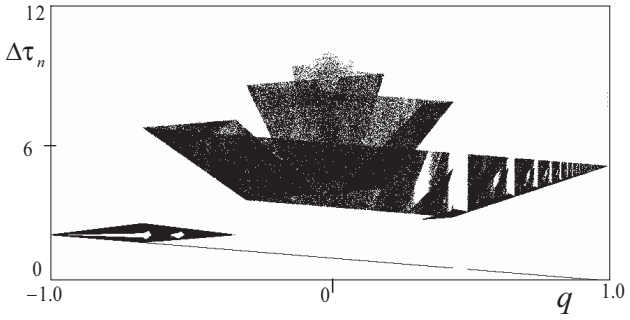

Figure 10: Distribution of the ISIs of the PWC-CSO for $a = 0.2$.

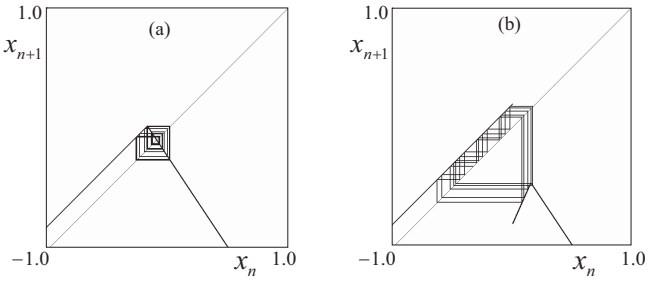

Figure 11: Typical return maps of the PWC-CSO for $a = 0.2$. (a) Chaos for $q = -0.81$, (b) Chaos for $q = 0.81$. Fig. (a) and (b) correspond to Fig. 8 (b) and (d).

[5] H. Hamanaka, H. Torikai and T. Saito, "Quantized spiking neuron with A/D conversion functions," IEEE Trans. Circuits Syst. II, 53, 10, pp. 1049-1053, 2006.

[6] H.Nakano and T.Saito, "Basic dynamics from an integrate-and-fire chaotic circuits with a periodic input," IEICE Trans. Fundamentals, E84-A, 5. pp.1293-1300, 2001.

[7] Y. Matsuoka and T. Saito, "A Simple Chaotic Spiking Oscillator Having Piecewise Constant Characteristics," IEICE Trans. Fundamentals, E89-A, 9, pp. 2437-2440, 2006.

[8] T.Tsubone and T.Saito, "Manifold piecewise constant systems and chaos," IEICE Trans. Fundamentals, E82-A, 8, pp.1619-1626, 1999.

[9] Y. Matsuoka, T. Hasegawa and T. Saito, "Chaotic Spike-train with Line-like Spectrum," IEICE Trans. Fundamentals, E92-A, 4, pp. 1142-1147, 2009.

[10] T. Hasegawa and T. Saito, "Bifurcation and Windows in a Simple Piecewise Linear Chaotic Spiking Neuron," Proc. of ICONIP, 2008.

[11] A. Lasota and M. C. Mackey, "Chaos, Fractals, and Noise - Second Edition," Springer-Verlag, 1994.